1 **Running Title:** *CCL22* upregulation in cancer cells via paracrine signaling

2

3 **Title:** *CCL22* is upregulated in cancer cells in response to paracrine signaling by STING-

4 activated myeloid cells

5

6 Elmira M Lomashvili[1], Jihyun Kim[1], Lingwei Kong[1], Pamela R. Cook[1]*

7 [1]Department of Biomedical Sciences, Mercer University School of Medicine, Macon, GA, USA

8 *Corresponding: Pamela R. Cook cook_p@mercer.edu

ABSTRACT

Solid tumors can evolve mechanisms that facilitate evasion of anti-tumor immune responses. Recruitment of regulatory T cells (Tregs) to the tumor microenvironment, which can inhibit cell-mediated immunity, represents one such strategy. A well-described mechanism of Treg recruitment occurs via the chemokine CCL22. Our lab and others have shown that CCL22 is upregulated in cancer cells via activation of the STimulator of INterferon Genes (STING). STING triggers robust immune responses against cytoplasmic DNA, which can accumulate in cancer cells due to chromosomal instability, damaged mitochondria, and increased expression of LINE-1 retrotransposons. LINE-1 is highly upregulated in many cancer types, and LINE-1 activation of STING in cancer cells may have clinically relevant outcomes on anti-tumor immunity. STING has been associated with both anti- and pro-tumor immune responses, and a potential mechanism of STING-mediated immune evasion is through CCL22 upregulation. CCL22 was first characterized in macrophages, and here we investigate the effects of STING activation on *CCL22* expression in macrophages and monocytes. We find that human macrophages and monocytes are resistant to *CCL22* upregulation by STING, but that STING-activated macrophages and monocytes release unidentified paracrine factor(s) that dramatically increase *CCL22* upregulation in cancer cells. This increase exceeds upregulation induced by direct, pharmacological activation of STING. Moreover, we found that the activity of the paracrine factors on *CCL22* requires intact STING in cancer cells, as evidenced by the inability of STING knockout cells to upregulate *CCL22* in response to these factors.

29 **INTRODUCTION**

30 The STimulator of INterferon Genes (STING) is an effector protein that transmits signals
31 from various cytosolic DNA sensors to downstream transcription factors, including interferon
32 regulatory factor 3 (IRF3), which robustly activates expression of type I interferon (*IFN*) genes
33 and downstream immune responses. (1-3). Healthy, non-mitotic eukaryotic cells confine DNA to
34 the nucleus and mitochondria; thus, the presence of cytosolic DNA often signals infection by
35 microbes, making STING an important sentinel in innate immune surveillance. Cancer cells are
36 often characterized by self-DNA mislocalized to the cytoplasm due to chromosomal instability,
37 damaged mitochondria, and reactivated LINE-1 retrotransposons (4, 5). LINE-1-mediated
38 activation of STING is thought to contribute to inflammation in multiple disease states, including
39 age-related neuropathologies and cancer (5-8). In the context of cancer, LINE-1 is robustly
40 expressed in many epithelial tumors (9-11), and its activation of STING in those cells may have
41 important clinical implications on host anti-tumor immune responses. STING activation in
42 cancer can boost anti-tumor immunity due to the release of type I IFNs, and indeed STING
43 agonists represent promising immunotherapy agents (12, 13). However, the roles of STING in
44 carcinogenesis, tumor progression, and metastasis are complex, and in some cases STING
45 activation has been associated with impaired anti-tumor immunity (14-16).

46 Our lab and others have demonstrated a link between STING activation and increased
47 expression of a chemokine associated with immunosuppression in the tumor microenvironment,
48 the C-C-motif ligand 22 (*CCL22*) (17-19). CCL22 recruits regulatory T-cells (Tregs) via its
49 interaction with the CCR4 receptor, which may reduce tumor immune responses and promote
50 immunosuppression in some cancers (20, 21). Correlations between *CCL22* expression and
51 adverse outcomes across various cancer types have been reported in multiple studies (18, 22-26),

52 although CCL22 has also been associated with increased patient survival in some cancers,
53 particularly for colon and head and neck squamous cell carcinomas (19 and references therein).
54 CCL22, also known as macrophage-derived chemokine (MDC), was originally
55 discovered in macrophages (27, 28). Given that macrophages are a major target of STING
56 agonists in the tumor microenvironment, we sought to investigate the relationship between
57 STING activation and *CCL22* upregulation in these cells. Although we found that STING
58 activation did not increase *CCL22* expression in macrophages or monocytes, we found that
59 factor(s) released from these myeloid cells dramatically upregulated *CCL22* in cancer cells in a
60 paracrine fashion. Moreover, we determined that this paracrine effect remains dependent on
61 STING in the cancer cells. We previously showed that *CCL22* upregulation in response to
62 STING activation occurs predominantly via the STING-IRF3 axis (19), the same axis that
63 triggers robust upregulation of type I IFNs. We thus hypothesized that type I IFNs could be the
64 relevant paracrine factor(s) released by myeloid cells that upregulate *CCL22* in cancer cells.
65 However, our results indicate that type I IFNs have only modest effects on *CCL22* in HeLa cells
66 compared to paracrine factors released from myeloid cells. And although MCF7 cells responded
67 more robustly to exogenous IFNβ than HeLa cells, the effect of paracrine factors released from
68 STING-activated monocytes was still larger; however, media from STING-activated
69 macrophages had somewhat less effect on *CCL22* in MCF7 cells compared to IFNβ. In
70 summary, this work shows that STING-activated macrophages and monocytes can dramatically
71 upregulate *CCL22* in cancer cells via paracrine signaling in a manner that is STING dependent in
72 the cancer cells and that appears to be mediated in some cases by factors other than type I IFNs.

73 **MATERIALS AND METHODS**

74

75 **Cells and cell culture**

76 Cell lines used in the study include MCF7 (human mammary gland adenocarcinoma), THP-1
77 (human monocytic leukemia), both purchased from ATCC, human HeLa cervical
78 adenocarcinoma cells, a kind gift from Dr. Anthony Furano from the National Institute of
79 Diabetes and Digestive and Kidney Diseases as described in (19), and HeLa$^{-/-TMEM173}$ STING
80 *(TMEM173)* knockout cells, engineered from the aforementioned wild type HeLa with the
81 CRISPR-Cas 9 system, also described in (19). All cells were cultured in DMEM high glucose
82 with GlutaMAX and pyruvate (Gibco, cat. 10569010) supplemented with 10% fetal bovine
83 serum (Gibco OneShot, non-heat-inactivated, cat. A3160401) and 1x antibiotic-antimycotic (100
84 units/mL penicillin, 100 ug/mL streptomycin, 0.25 ug/mL Amphotericin B; Gibco, cat.
85 15240096) in a humidified incubator at 37°C with 5% CO_2. THP-1 culture media was
86 additionally supplemented with 1x 2-mercaptoethanol (Gibco, cat. 21985023).

87

88 **Cell culture treatments (STING agonists, IFNα, IFNβ, and MMHAR-2 block)**

89 Four commercially available STING agonists were used in the study: a stabilized analog of the
90 cyclic dinucleotide canonical STING agonist 2'3'-cGAMP (2'3'-cGAM(PS)2(Rp/Sp)), hereafter
91 referred to as cGAM(PS)2 (Invivogen, cat. tlrl-nacga2srs), a stabilized cyclic adenine
92 monophosphate-inosine monophosphate (cAIM(PS)2 Difluor (Rp/Sp), hereinafter referred to as
93 cAIM(PS)2 (Invivogen, cat. tlrl-nacairs-2), E7766, a macrocycle-bridged diammonium salt
94 (Chemietek, cat. CT-E7766), and the diamidobenzimidazole diABZI (Selleckchem, cat.
95 S8796). All agonists except diABZI were water soluble and reconstituted using a companion

96 vial of sterile, endotoxin-free LAL water; diABZI was reconstituted in dimethyl sulfoxide
97 (DMSO). All agonists were diluted to a final concentration of 30 uM in complete cell culture
98 media and applied to cells as specified in the figures. Human recombinant IFNα stock (pbl assay
99 science, cat. 11101-1) was diluted to concentrations indicated in the figure legends in complete
100 cell culture media. Lyophilized recombinant human IFNb (PeproTech, cat. 300-02) was initially
101 reconstituted in sterile, endotoxin-free LAL water and further diluted into sterile 0.1% bovine
102 serum albumin (BSA) in 1x phosphate-buffered saline (PBS) to 100 ng/uL and further diluted to
103 concentrations indicated in the figure legends in complete cell culture media before adding to
104 cells. MMHAR-2 blockade was performed by pretreating cells with 8.3 µg/mL of the MMHAR-
105 2 antibody, then adding indicated treatments diluted in cell culture media, reducing the final
106 concentration of MMHAR-2 to 5 µg/mL. Cells were then incubated for approximately 30 hours
107 prior to harvesting for either Western blots or RTqPCR.
108
109 **Macrophage differentiation and generation of conditioned media**
110 THP-1 cells were differentiated into macrophages by plating cells in complete culture media
111 supplemented with 150 nM phorbol 12-myristate 13-acetate (PMA) and incubating for 96 hours,
112 with one media change performed after 48 hours to replenish PMA. PMA-containing media was
113 then removed, and cells were allowed to rest for 24 hours prior to treatment with cGAM(PS)2.
114 Conditioned media from both macrophages and undifferentiated monocytes was obtained by
115 treating cells with fresh complete media, with or without the addition of 30 uM cGAM(PS)2,
116 incubating for 24 hours, then gently removing media, centrifuging at 300 x g, and transferring to
117 cancer cells.
118

119 **Cell imaging**

120 The morphological changes during THP-1 differentiation were imaged using an EVOS FLoid
121 system.

122

123 **RNA purification and RTqPCR**

124 Cells were harvested using TRIzol reagent (Invitrogen, cat. 15596026) followed by column RNA
125 purification and on-column DNase digestion according to the TRIzol two-step protocol from the
126 Monarch total RNA miniprep kit (NEB, cat. T2010S). Purity and concentration of the RNA were
127 assessed using spectrophotometry. First-strand cDNA synthesis was performed using the
128 LunaScript RT SuperMix Kit (NEB, cat. E3010S) or LunaScript (-) RT SuperMix control with
129 added M-MuLV Reverse Transcriptase (NEB). qPCR was performed on a QuantStudio 3 real-
130 time PCR machine using TaqMan Fast Advanced Master Mix (Applied Biosystems, cat.
131 A44359). Singleplexed and duplexed 5' endonuclease assays were performed using the
132 following TaqMan Assays: *CCL22* (Hs00171080); IFN-β (Hs01077958_s1; beta actin
133 (Hs99999903); and 18s (Hs99999901). For duplexed assays, a beta-actin primer-limited assay
134 (IDT) was used. Samples for qPCR were assayed in technical triplicates, and data were analyzed
135 with the delta-delta Ct method; when multiple housekeeping genes were measured, their
136 combined geometric mean was used for analysis.

137

138 **Cell lysis and Western blotting**

139 Cells were lysed for immunoblotting in 3% SDS, 25 mM Tris-HCl pH 7.4, and 0.5 mM EDTA
140 supplemented with 3X HALT protease and phosphatase inhibitor cocktail (ThermoFisher, cat.
141 78440). Lysate homogenization was achieved with QIAshredder columns (Qiagen, cat. 79656),

142 after which protein concentration was determined using the BioRad DC Protein Assay (cat.
143 5000112). Equal amounts of lysates were resolved with SDS-PAGE. Transfers were performed
144 using a wet tank system overnight at 28 V or the BioRad Trans-Blot Turbo Transfer system.
145 Blots were imaged with an infrared Li-Cor Odyssey CLx Imager and processed using Image
146 Studio (Li-Cor). Positive controls for phospho-STING (S366) were prepared as commercially
147 described by transfecting THP-1 differentiated macrophages with dsDNA (pcDNA3.1 (+) puro),
148 (3.33 ug/mL) using Opti-MEM (Gibco, cat. 31-985-062) as the DNA diluent and TransIT-LT1
149 (Mirus, cat. MIR 2300) at a ratio of 1 ug DNA: 2 uL TransIT-LT1; cells were harvested 4 hours
150 after transfection with the lysis buffer described above.
151
152 **Antibodies**
153 Antibodies for Western blots included: anti-phospho(S366)-STING (Cell Signaling Technology,
154 cat. 19781S); anti-phospho(Y701)-Stat1 (Cell Signaling Technology, cat. 9167); anti-IFNAR2
155 (Cell Signaling Technology, cat. 53883); and anti-beta-tubulin (Abcam, cat. ab6046). The
156 antibody used for IFNAR blockade was anti-human interferon alpha/beta receptor chain 2, clone
157 MMHAR-2 (pbl assay science, cat. 21385-1).
158
159 **Statistical analyses**
160 Statistical analyses were performed using GraphPad Prism 9. Tests for significance are described
161 in the figure legends, and statistical significance was defined as p-value ≤ 0.05.
162

163 **RESULTS**

164

165 **STING activation in macrophages and monocytes does not upregulate *CCL22*.** Macrophages
166 are a major source of CCL22, reflected in the historical eponymous name of CCL22,
167 macrophage-derived chemokine (MDC). Since one of the targets of STING agonists are tumor-
168 associated macrophages, we sought to determine the effect of STING activation on *CCL22* in
169 these cells. Using the well-established THP-1 monocyte-to-macrophage differentiation model
170 (Fig. 1A), we incubated THP-1 monocytes with phorbol myristate acetate (PMA) for four days to
171 establish adherent, differentiated macrophages. Following differentiation, we treated the THP-1-
172 derived macrophages with the canonical human STING agonist cGAM(PS)2 for 24 hours.
173 Surprisingly, we found that cGAM(PS)2 did not increase *CCL22* expression but rather reduced it
174 (Fig. 1B). To ensure that we had not missed an increase in *CCL22* at an earlier time point, we
175 monitored *CCL22* expression at 0, 6, 12, 24, and 48 hours, which revealed no significant increase
176 at any time point (Fig. S1). Rather, the time course in Fig. S1 shows a downward trend in *CCL22*
177 expression at each time point, although these decreases did not reach statistical significance in
178 the context of a Kruskal-Wallis multiple comparisons test, which generally has less power to
179 identify differences in means compared with the *t* test used to analyze data in Figure 1B. Indeed,
180 when analyzing only the 24-hour time-course data with an unpaired, two-tailed *t* test, the
181 decrease in *CCL22* was again significant ($p = 0.0290$). To determine whether failure to activate
182 *CCL22* in macrophages was due to a lack of STING activation, we confirmed that cGAM(PS)2
183 induced STING phosphorylation in macrophages at both 6 and 24 hour time points (Fig. 1C).
184 Consistent with results from macrophages, undifferentiated THP-1 monocytes also failed to
185 upregulate *CCL22* in response to cGAM(PS)2 (Fig. 1D). The absence of *CCL22* upregulation in

186 response to STING activation in THP-1 monocytes and macrophages was completely
187 unexpected and in contrast to previous work by us and others showing that STING activation in
188 cancer cells increases *CCL22* expression (17-19).
189
190 **STING-activated macrophages and monocytes release factor(s) that upregulate *CCL22* in**
191 **cancer cells.** Macrophages have important roles in anti-tumor immunity but can also contribute
192 to immunosuppressive environments (29). We thus sought to determine whether STING-
193 activated macrophages might release factors that could act via paracrine signaling to alter *CCL22*
194 expression in cancer cells. *CCL22* has been reported to play a role in breast (22, 24, 26) and
195 cervical (18, 25) cancers, and we used human breast (MCF7) and cervical (HeLa) cancer cells in
196 these experiments. These cell lines were also used in our previous study, where we showed that
197 both CCL22 mRNA and protein were increased upon direct STING activation with cytosolic
198 DNA or cGAM(PS)2 (19). To investigate potential paracrine activation of *CCL22* in these cells,
199 we first treated macrophages with cGAM(PS)2 or a mock control for 24 hours, then removed the
200 media and applied it to cancer cells for 24 hours. Both MCF7 (Fig. 2A) and HeLa cells (Fig. 2B)
201 exposed to conditioned media from macrophages treated with cGAM(PS)2 exhibited a robust
202 increase in *CCL22* compared to media from untreated macrophages or treatment with
203 cGAM(PS)2 alone, although conditioned media from untreated macrophages also increased
204 *CCL22* in HeLa cells, albeit to a lower extent. Monocytes also released factors that increased
205 *CCL22* above levels induced by direct STING activation in MCF7 (Fig. 2C) and HeLa (Fig. 2D)
206 cells.
207

208 **Paracrine activation of *CCL22* remains dependent on STING.** Our previous study showed
209 that *CCL22* upregulation in response to cytosolic dsDNA and cGAM(PS)2 in HeLa cells was
210 dependent on STING. However, in the current experiments, it was possible that paracrine-
211 mediated activation of *CCL22* in these cells was independent of STING. To investigate this, we
212 first determined whether conditioned media from STING-activated macrophages had any effect
213 on STING activation in HeLa cells, as determined by analysis of STING phosphorylation on
214 serine 366 (30, 31). Figure 3A shows that STING in HeLa cells was indeed activated by media
215 obtained from STING-activated macrophages, and this activation was greater than when HeLa
216 cells were treated directly with cGAM(PS)2. Importantly, in our previous study, we confirmed
217 that free-floating DNA, which could possibly have been present in the conditioned media, did
218 not activate STING in HeLa cells (19). Notably, the degree of STING activation by each
219 treatment in Figure 3A generally corresponds to relative levels of *CCL22* upregulation in Figure
220 2B, including the slight increases observed in response to media from untreated macrophages.
221 Similar results for STING phosphorylation were observed when treating HeLa cells with
222 conditioned media from monocytes (Fig. S2A), which again parallels increases in *CCL22* in
223 Figure 2D. Note that we did not examine STING phosphorylation on S366 in MCF7 cells due to
224 our previous finding that STING activation in MCF7 cells with cytosolic dsDNA or
225 pharmacological agonists occurred in the absence of phosphorylation on S366 for unknown
226 reasons, which are further discussed in that study (19). To determine whether the observed
227 STING activation was *required* for paracrine-mediated upregulation of *CCL22*, we used a
228 STING (gene name *TMEM173*) knockout cell line, HeLa$^{-/-TMEM173}$, which we previously
229 established and characterized from the parental HeLa cells used here (19). Treatment of the
230 HeLa$^{-/-TMEM173}$ STING knockout cells with media from STING-activated macrophages showed

231 no statistically significant increase in *CCL22* expression, indicating that intact STING signaling
232 in the cancer cells was still required for upregulated *CCL22* (Fig. 3B). Similar results were
233 obtained using media from STING-activated monocytes (Fig. S2B).
234
235 **Type I IFNs have modest effects on *CCL22* in HeLa cells that remain STING-dependent.**
236 We previously found that STING-mediated *CCL22* upregulation in HeLa cells is mediated
237 predominantly via the STING-IRF3 axis, which triggers robust expression of type I IFNs (19).
238 We therefore hypothesized that the relevant paracrine factor(s) leading to the increase in *CCL22*
239 might be type I IFNs. Overall however, IFNα failed to elicit strong *CCL22* expression in either
240 cell type, and effects of IFNβ plateaued in dose-response curves, indicating that the relevant
241 paracrine factor was unlikely a higher concentration of type I IFNs.
242 In HeLa cells, IFNβ did not significantly upregulate *CCL22* at any dose at 24 hours (Fig.
243 S3A), and subsequent time-course analyses indicated the maximum response to both IFNα and
244 IFNβ occurred at 48 hours. However, even at 48 hours, IFNα failed to significantly upregulate
245 *CCL22* in HeLa cells except at the highest dose (100 ng/mL), and then only to an average of 15
246 fold (Fig. 4A). IFNβ increased *CCL22* at the lowest dose (1 ng/mL) in HeLa cells, but only to
247 approximately 10 fold, and higher doses of IFNβ failed to elicit any additional increase (Fig. 4B).
248 MCF7 cells upregulated CCL22 in response to type I IFNs more rapidly than HeLa cells,
249 showing higher levels at 24 hours compared to 48 hours (Fig. S3B). At the highest dose, IFNα
250 increased *CCL22* by an average of only 6.7 fold in 24 hours (Fig. 4C). Paralleling the relative
251 effects of IFNα and IFNβ in HeLa cells, IFNβ also increased *CCL22* in MCF7 cells more than
252 IFNα, with an average of 57 fold change in 24 hours at the highest dose (Fig. 4D). However, the
253 effect of IFNβ was still below that observed from paracrine activation of MCF7 cells by

254 conditioned media from STING-activated monocytes (76.5 fold, Fig. 2C) but slightly above
255 levels induced by conditioned media from STING-activated macrophages (46.3 fold, Fig. 2A).
256 We next tested the effect of exogenous IFNα and IFNβ on *CCL22* upregulation in the
257 context of STING knockout cells, HeLa$^{-/-TMEM173}$. Surprisingly, neither IFNα (Fig. 4E) nor IFNβ
258 (Fig. 4F) significantly affected *CCL22* expression in STING knockout cells. These data were
259 unexpected and indicate that the effect of exogenous IFNα and IFNβ on *CCL22* is dependent on
260 STING. Although STING is well-known to trigger expression of type I *IFNs* downstream of
261 IRF3, to our knowledge, activation of STING by exogenous type I IFNs has not been reported
262 and suggests unrealized crosstalk between them. To confirm that STING was activated by type I
263 IFN signaling, we treated wild-type HeLa cells with IFNβ and then performed a Western blot to
264 assess STING phosphorylation (Fig. 4G). We did not test the effect of IFNα due to the
265 comparatively minimal effect we observed from IFNα on *CCL22* relative to IFNβ. To rule out
266 the possibility that type I IFNs failed to upregulate *CCL22* in the STING KO cells due to an
267 inadvertent disruption of the interferon receptor (IFNAR) and downstream Stat1 signaling, we
268 confirmed that our STING KO cells exhibited the same degree of Stat1 phosphorylation in
269 response to IFNα and IFNβ as wild type cells (Fig. 4H). As expected, we found that
270 cGAM(PS)2, which activates STING and STING-mediated type I IFNs, also slightly induced
271 Stat1 in the wild type cells, but this activation was blocked in the STING KO cells, reflecting the
272 lack of STING-mediated upregulation of type I IFNs available to bind and activate the IFNAR-
273 Stat1 pathway in those cells (Fig. 4H). Given that Stat1 phosphorylation was equivalently
274 induced in wild type and STING knockout cells by type I IFNs, it was unlikely that IFNAR
275 expression would have been reduced in the STING knockout cells, but to confirm this, we also
276 show equivalent levels of IFNAR in both cell lines (S3C).

277 The inability of type I IFNs to activate *CCL22* expression in our STING KO cells,
278 combined with confirmation of intact IFNAR expression and signaling in STING KO cells,
279 indicated that *CCL22* upregulation in wild type cells by type I IFNs occurs via STING. To
280 further examine the role of IFNAR signaling on *CCL22* activation in the context of type I IFNs,
281 direct STING activation with cGAM(PS)2, or paracrine activation using conditioned media, we
282 performed an IFNAR blockade using a well-characterized neutralizing monoclonal antibody
283 from PBL Assay Science, anti-human IFN-alpha/beta receptor chain 2, clone MMHAR-2. To
284 first confirm that MMHAR-2 exerted a neutralizing effect on IFNAR signaling, we analyzed the
285 ability of this antibody to reduce Stat1 phosphorylation in response to IFNα and IFNβ, as well as
286 cGAM(PS)2. MMHAR-2 somewhat reduced levels of phosphorylated Stat1 in response to
287 IFNα, but not IFNβ (Fig. S3D). This difference might be attributable to the reported higher
288 affinity of IFNβ for IFNARs compared to IFNα (32, 33). Given that cGAM(PS)2 upregulates
289 type I IFNs through its activation of STING, we observed as expected that the MMHAR-2
290 blockade also reduced Stat1 phosphorylation following treatment with cGAM(PS)2 (Fig. S3D).
291 We also confirmed that MMHAR-2 exerted no activating effect on Stat1 (Fig. S3E). After
292 establishing the neutralizing potential of MMHAR-2 in our system, we sought to determine the
293 contribution of IFNAR signaling to *CCL22* upregulation in response to type I IFNs,
294 cGAM(PS)2, and paracrine factors from STING-activated macrophages. Figure 4I shows the
295 relative degree of inhibition induced by MMHAR-2 for each treatment. Although not statistically
296 significant, MMHAR-2 produced an observable downward trend in *CCL22* expression for all
297 treatments except cGAM(PS)2. The neutralizing effect of MMHAR-2 was most noticeable in
298 cells treated with IFNα, where the p-value is approaching significance at 0.0659, and these
299 results parallel those observed for MMHAR-2 inhibition of IFNα-mediated Stat1

300 phosphorylation in Figure S3D. Also in Figure S3D, the very slight increase in Stat1
301 phosphorylation from cGAM(PS)2 treatment, as well as its return to baseline with MMHAR-2
302 pretreatment, most likely reflects the activity of cGAM(PS)2-induced type I IFNs downstream of
303 STING; however, the IFNAR block had the least effect on *CCL22* upregulation by cGAM(PS)2,
304 further indicating that *CCL22* upregulation downstream of STING in HeLa cells is not mediated
305 primarily or solely by type I IFNs.
306
307 **STING agonists differentially upregulate *CCL22* and *IFNβ***
308 We were curious, given the differential effects of type I IFNs and cGAM(PS)2 on *CCL22,*
309 whether STING-mediated *IFNβ* upregulation and *CCL22* were correlated. We tested a panel
310 STING agonists that consisted of two cyclic dinucleotides, cGAM(PS)2 and the stabilized analog
311 of adenosine-inosine monophosphate (cAIMP(PS)2) (34, 35), and two non-cyclic dinucleotides,
312 diamidobenzimidazole (diABZI) (36-38) and E7766, a locked, macrocycle-bridged agonist (37,
313 39, 40). In HeLa cells, all agonists increased *CCL22* but had no significant effect on *IFNβ*
314 expression (Fig. 5A-5D). STING agonist treatment of MCF7 cells also generally resulted in
315 higher levels of *CCL22* compared with *IFNβ* (Fig. 5E-5H), although the data spread in
316 cAIM(PS)2 treated MCF7 cells (Fig. 5F) resulted in failed significance for both *CCL22* and
317 *IFNβ*. Correlation analysis for experiments where both *CCL22* and *IFNβ* were significantly
318 increased in MCF7 cells showed no direct relationship between STING-induced *IFNβ* levels and
319 *CCL22* (Fig. 5I), consistent with our other data indicating that STING-mediated upregulation of
320 *CCL22* does not occur primarily via type I IFNs.
321
322

323 **DISCUSSION**

324 Complex intercellular crosstalk within the tumor microenvironment can contribute to
325 immune evasion. CCL22 has been implicated in tumor immune evasion via recruitment of
326 regulatory T cells (20, 21), and both STING (41) and CCL22 (42) are implicated in the
327 polarization of macrophages towards a more pro-tumor phenotype. We previously showed that
328 epithelial cancer cells treated with cytosolic DNA or the STING agonist cGAM(PS)2 can
329 upregulate expression of *CCL22* (19). Although few studies have investigated the connection
330 between STING and *CCL22*, a growing body of evidence suggests that STING-mediated
331 activation of *CCL22* may play a role in multiple cancers (17, 18). In addition to the potential
332 effects of CCL22 in cancer immunity, it is possible that CCL22 upregulation downstream of
333 STING may represent a general conserved pathway in modulating inflammation, as unchecked
334 STING activity has been associated with a range of autoimmune and inflammatory diseases (43,
335 44).

336 In the present study, we show that macrophages, which are important components of
337 tumor microenvironments and *in vivo* targets of STING agonists, do not themselves upregulate
338 *CCL22* in response to STING activation, but rather release unidentified factor(s) that in turn
339 increase *CCL22* expression in a paracrine fashion in cancer cells. In addition to macrophages, we
340 found the same paracrine mechanism elicited from STING-activated monocytes. A similar
341 observation was made by Faget et al., who showed that co-culture of PBMCs and breast tumor
342 cells led to increased production of CCL22 by the later and recruitment of Tregs, and that
343 purified monocytes and exogenous interferon gamma (IFN-γ) could also promote CCL22
344 production by breast cancer cells (45). Our finding that STING activation in macrophages and
345 monocytes induces paracrine factors that drive *CCL22* expression from cancer cells adds

346 important new mechanistic insights into how tumor-associated cells may facilitate Treg
347 recruitment. Notably, we found that STING-induced paracrine activation resulted in higher
348 levels of *CCL22* in HeLa cells than direct treatment of the cells with STING agonists. As stated,
349 we considered that these paracrine factors might be type I IFNs, based on our previous study that
350 showed *CCL22* upregulation by STING in HeLa cells occurs predominantly via the STING-IRF3
351 pathway. However, our present work indicates that type I IFNs have minimal effect on *CCL22*
352 expression in HeLa cells. Exogenous type I IFN dose-response curves indicated that *CCL22*
353 upregulation plateaued at 10 – 20 fold, compared with up to 8,000 fold in response to paracrine
354 factors released by STING-activated macrophages, as shown in Figure 2B. Also arguing against
355 a direct effect of type I IFNs on *CCL22* is a previous study reporting that treatment of human
356 oral squamous carcinoma HSC-3 cells with either poly(dA:dT) or the STING agonist 2'-3'
357 cGAM(PS)2 induced upregulation of IFNβ by approximately 500 and 12 fold, respectively, but
358 had essentially the same effects on *CCL22* mRNA upregulation at ~ 8 fold in both cases (17).
359 However, we also show here that MCF7 cells, in contrast to HeLa cells, respond more robustly
360 to exogenous type I IFNs and less strongly to conditioned media from STING-activated myeloid
361 cells, highlighting our and others previous reports of cell-type specificity with respect to *CCL22*
362 regulation (19).
363 Surprising, we found that the effect of exogenous type I IFNs on *CCL22* was STING-
364 dependent. Although STING-dependent expression of type I IFNs is well-described, a
365 requirement for STING for a functional effect of exogenous type I IFNs has, to our knowledge,
366 not been reported. One possible explanation could be our finding that IFNβ itself induces
367 activating phosphorylation of STING, which also has not previously been reported. However,
368 other studies have shown connections between type I IFNs and the transcriptional regulation of

369 STING: IFNα is reported to induce transcription of both *cGAS* and *TMEM173,* and IFNβ has
370 been shown to increase binding of the Stat1 transcription factor to the promoters of *cGAS* and
371 *TMEM173* (46, 47). Taken together, these findings raise important questions regarding feedback
372 mechanisms between type I IFNs and STING.

373 This study increases our understanding of the complex crosstalk and potential
374 mechanisms that can shift the balance between anti-tumor immunity and immune evasion.
375 However, our work also raises questions regarding the paracrine factor(s) released from STING-
376 activated myeloid cells. Faget et al. identified roles for TNF-α, INF-γ, and IL-1β in the increase
377 of CCL22 in breast cancer cells (45), but whether these are the relevant paracrine factors
378 produced from STING-activated monocytes and macrophages, and whether their action on
379 CCL22 in cancer cells is also dependent on STING, remains unknown. Identification of STING-
380 induced paracrine factor(s) could reveal novel therapeutic options to reduce *CCL22* and Treg
381 accumulation in solid tumors, especially in the context of treatment with STING agonists. One
382 potential candidate is cGAMP itself, which can be generated and released from various cell
383 types, including macrophages, and has been shown to function as a secreted, intercellular
384 immunotransmitter (4, 48-52). Another likely possibility is that a combination of multiple factors
385 synergistically activate STING in cancer cells to drive CCL22 production. Additional studies
386 will be needed to unravel the intercellular mechanisms of STING-dependent paracrine activation
387 of CCL22 in cancer cells.
388

389 **REFERENCES**

390 1. Zhang, B., P. Xu, and A. Ablasser. 2025. Regulation of the cGAS-STING Pathway. *Annu*
391 *Rev Immunol* 43: 667-692.

392 2. Motwani, M., S. Pesiridis, and K. A. Fitzgerald. 2019. DNA sensing by the cGAS-
393 STING pathway in health and disease. *Nat Rev Genet* 20: 657-674.

394 3. Hopfner, K. P., and V. Hornung. 2020. Molecular mechanisms and cellular functions of
395 cGAS-STING signalling. *Nat Rev Mol Cell Biol* 21: 501-521.

396 4. Dvorkin, S., S. Cambier, H. E. Volkman, and D. B. Stetson. 2024. New frontiers in the
397 cGAS-STING intracellular DNA-sensing pathway. *Immunity* 57: 718-730.

398 5. Mathavarajah, S., and G. Dellaire. 2024. LINE-1: an emerging initiator of cGAS-STING
399 signalling and inflammation that is dysregulated in disease. *Biochem Cell Biol* 102: 38-
400 46.

401 6. Gamdzyk, M., D. M. Doycheva, C. Araujo, U. Ocak, Y. Luo, J. Tang, and J. H. Zhang.
402 2020. cGAS/STING Pathway Activation Contributes to Delayed Neurodegeneration in
403 Neonatal Hypoxia-Ischemia Rat Model: Possible Involvement of LINE-1. *Mol Neurobiol*
404 57: 2600-2619.

405 7. Gorbunova, V., A. Seluanov, P. Mita, W. McKerrow, D. Fenyo, J. D. Boeke, S. B.
406 Linker, F. H. Gage, J. A. Kreiling, A. P. Petrashen, T. A. Woodham, J. R. Taylor, S. L.
407 Helfand, and J. M. Sedivy. 2021. The role of retrotransposable elements in ageing and
408 age-associated diseases. *Nature* 596: 43-53.

409 8. De Cecco, M., T. Ito, A. P. Petrashen, A. E. Elias, N. J. Skvir, S. W. Criscione, A.
410 Caligiana, G. Brocculi, E. M. Adney, J. D. Boeke, O. Le, C. Beauséjour, J. Ambati, K.
411 Ambati, M. Simon, A. Seluanov, V. Gorbunova, P. E. Slagboom, S. L. Helfand, N.
412 Neretti, and J. M. Sedivy. 2019. L1 drives IFN in senescent cells and promotes age-
413 associated inflammation. *Nature* 566: 73-78.

414 9. Rodic, N., R. Sharma, R. Sharma, J. Zampella, L. Dai, M. S. Taylor, R. H. Hruban, C. A.
415 Iacobuzio-Donahue, A. Maitra, M. S. Torbenson, M. Goggins, M. Shih Ie, A. S. Duffield,
416 E. A. Montgomery, E. Gabrielson, G. J. Netto, T. L. Lotan, A. M. De Marzo, W. Westra,
417 Z. A. Binder, B. A. Orr, G. L. Gallia, C. G. Eberhart, J. D. Boeke, C. R. Harris, and K. H.
418 Burns. 2014. Long interspersed element-1 protein expression is a hallmark of many
419 human cancers. *Am J Pathol* 184: 1280-1286.

420 10. Burns, K. H. 2017. Transposable elements in cancer. *Nat Rev Cancer* 17: 415-424.

421 11. McKerrow, W., N. Doudican, N. Frazzette, S. A. Evans, A. Rocha, L. Kagermazova, J.
422 M. Sedivy, N. Neretti, J. Carucci, J. D. Boeke, and D. Fenyö. 2022. LINE-1
423 Retrotransposon expression in cancerous, epithelial and neuronal cells revealed by 5'
424 single-cell RNA-Seq. *bioRxiv*: 2021.2001.2019.427347.

425 12. Gan, Y., X. Li, S. Han, Q. Liang, X. Ma, P. Rong, W. Wang, and W. Li. 2021. The
426 cGAS/STING Pathway: A Novel Target for Cancer Therapy. *Front Immunol* 12: 795401.

427 13. Xu, Y., and Y. Xiong. 2024. Targeting STING signaling for the optimal cancer
428 immunotherapy. *Front Immunol* 15: 1482738.

429 14. Zhou, Z., S. Huang, F. Fan, Y. Xu, C. Moore, S. Li, and C. Han. 2024. The multiple faces
430 of cGAS-STING in antitumor immunity: prospects and challenges. *Med Rev (2021)* 4:
431 173-191.

432 15. Samson, N., and A. Ablasser. 2022. The cGAS-STING pathway and cancer. *Nat Cancer*
433 3: 1452-1463.

434 16. Yue, B., W. Gao, J. F. Lovell, H. Jin, and J. Huang. 2025. The cGAS-STING pathway in
435 cancer immunity: dual roles, therapeutic strategies, and clinical challenges. *Essays*
436 *Biochem* 69.

437 17. Liang, D., H. Xiao-Feng, D. Guan-Jun, H. Er-Ling, C. Sheng, W. Ting-Ting, H. Qin-
438 Gang, N. Yan-Hong, and H. Ya-Yi. 2015. Activated STING enhances Tregs infiltration
439 in the HPV-related carcinogenesis of tongue squamous cells via the c-jun/CCL22 signal.
440 *Biochim Biophys Acta* 1852: 2494-2503.

441 18. Ni, H., H. Zhang, L. Li, H. Huang, H. Guo, L. Zhang, C. Li, J. X. Xu, C. P. Nie, K. Li, X.
442 Zhang, X. Xia, and J. Li. 2022. T cell-intrinsic STING signaling promotes regulatory T
443 cell induction and immunosuppression by upregulating FOXP3 transcription in cervical
444 cancer. *J Immunother Cancer* 10.

445 19. Kim, J., J. V. Pena, H. P. McQueen, L. Kong, D. Michael, E. M. Lomashvili, and P. R.
446 Cook. 2024. Downstream STING pathways IRF3 and NF-kappaB differentially regulate
447 CCL22 in response to cytosolic dsDNA. *Cancer Gene Ther* 31: 28-42.

448 20. Anz, D., M. Rapp, S. Eiber, V. H. Koelzer, R. Thaler, S. Haubner, M. Knott, S. Nagel, M.
449 Golic, G. M. Wiedemann, F. Bauernfeind, C. Wurzenberger, V. Hornung, C. Scholz, D.
450 Mayr, S. Rothenfusser, S. Endres, and C. Bourquin. 2015. Suppression of intratumoral
451 CCL22 by type i interferon inhibits migration of regulatory T cells and blocks cancer
452 progression. *Cancer Res* 75: 4483-4493.

453 21. Sugiyama, D., H. Nishikawa, Y. Maeda, M. Nishioka, A. Tanemura, I. Katayama, S.
454 Ezoe, Y. Kanakura, E. Sato, Y. Fukumori, J. Karbach, E. Jager, and S. Sakaguchi. 2013.
455 Anti-CCR4 mAb selectively depletes effector-type FoxP3+CD4+ regulatory T cells,
456 evoking antitumor immune responses in humans. *Proc Natl Acad Sci U S A* 110: 17945-
457 17950.

458 22. Gobert, M., I. Treilleux, N. Bendriss-Vermare, T. Bachelot, S. Goddard-Leon, V. Arfi, C.
459 Biota, A. C. Doffin, I. Durand, D. Olive, S. Perez, N. Pasqual, C. Faure, I. Ray-Coquard,
460 A. Puisieux, C. Caux, J. Y. Blay, and C. Ménétrier-Caux. 2009. Regulatory T cells
461 recruited through CCL22/CCR4 are selectively activated in lymphoid infiltrates
462 surrounding primary breast tumors and lead to an adverse clinical outcome. *Cancer Res*
463 69: 2000-2009.

464 23. Lecoq, I., K. L. Kopp, M. Chapellier, P. Mantas, E. Martinenaite, M. Perez-Penco, L.
465 Ronn Olsen, M. B. Zocca, A. Wakatsuki Pedersen, and M. H. Andersen. 2022. CCL22-
466 based peptide vaccines induce anti-cancer immunity by modulating tumor
467 microenvironment. *Oncoimmunology* 11: 2115655.

468 24. Li, Y. Q., F. F. Liu, X. M. Zhang, X. J. Guo, M. J. Ren, and L. Fu. 2013. Tumor secretion
469 of CCL22 activates intratumoral Treg infiltration and is independent prognostic predictor
470 of breast cancer. *PLoS One* 8: e76379.

471 25. Wang, Q., E. Schmoeckel, B. P. Kost, C. Kuhn, A. Vattai, T. Vilsmaier, S. Mahner, D.
472 Mayr, U. Jeschke, and H. H. Heidegger. 2019. Higher CCL22+ Cell Infiltration is
473 Associated with Poor Prognosis in Cervical Cancer Patients. *Cancers (Basel)* 11.

474 26. Wiedemann, G. M., M. M. Knott, V. K. Vetter, M. Rapp, S. Haubner, J. Fesseler, B.
475 Kuhnemuth, P. Layritz, R. Thaler, S. Kruger, S. Ormanns, D. Mayr, S. Endres, and D.
476 Anz. 2016. Cancer cell-derived IL-1alpha induces CCL22 and the recruitment of
477 regulatory T cells. *Oncoimmunology* 5: e1175794.

478 27. Mantovani, A., P. A. Gray, J. Van Damme, and S. Sozzani. 2000. Macrophage-derived
479 chemokine (MDC). *J Leukoc Biol* 68: 400-404.

480 28. Yamashita, U., and E. Kuroda. 2002. Regulation of macrophage-derived chemokine
481 (MDC, CCL22) production. *Crit Rev Immunol* 22: 105-114.

482 29. Jung, M., and B. Bonavida. 2024. Immune Evasion in Cancer Is Regulated by Tumor-
483 Asociated Macrophages (TAMs): Targeting TAMs. *Crit Rev Oncog* 29: 1-17.

484 30. Liu, S., X. Cai, J. Wu, Q. Cong, X. Chen, T. Li, F. Du, J. Ren, Y. T. Wu, N. V. Grishin,
485 and Z. J. Chen. 2015. Phosphorylation of innate immune adaptor proteins MAVS,
486 STING, and TRIF induces IRF3 activation. *Science* 347: aaa2630.

487 31. Zhang, C., G. Shang, X. Gui, X. Zhang, X. C. Bai, and Z. J. Chen. 2019. Structural basis
488 of STING binding with and phosphorylation by TBK1. *Nature* 567: 394-398.

489 32. Lavoie, T. B., E. Kalie, S. Crisafulli-Cabatu, R. Abramovich, G. DiGioia, K. Moolchan,
490 S. Pestka, and G. Schreiber. 2011. Binding and activity of all human alpha interferon
491 subtypes. *Cytokine* 56: 282-289.

492 33. Schreiber, G. 2017. The molecular basis for differential type I interferon signaling. *The*
493 *Journal of Biological Chemistry* 292: 7285-7294.

494 34. Andersen, A. H. F., R. Olesen, K. L. Jonsson, J. F. Hojen, C. Krapp, K. Mack, M. K.
495 Thomsen, L. Ostergaard, M. Tolstrup, F. Dagnaes-Hansen, M. R. Jakobsen, and P. W.
496 Denton. 2019. cAIMP administration in humanized mice induces a chimerization-level-
497 dependent STING response. *Immunology* 157: 163-172.

498 35. Skouboe, M. K., A. Knudsen, L. S. Reinert, C. Boularan, T. Lioux, E. Perouzel, M. K.
499 Thomsen, and S. R. Paludan. 2018. STING agonists enable antiviral cross-talk between
500 human cells and confer protection against genital herpes in mice. *PLoS Pathog* 14:
501 e1006976.

502 36. Guerini, D. 2022. STING Agonists/Antagonists: Their Potential as Therapeutics and
503 Future Developments. *Cells* 11.

504 37. Motedayen Aval, L., J. E. Pease, R. Sharma, and D. J. Pinato. 2020. Challenges and
505 Opportunities in the Clinical Development of STING Agonists for Cancer
506 Immunotherapy. *J Clin Med* 9.

507 38. Su, T., Y. Zhang, K. Valerie, X. Y. Wang, S. Lin, and G. Zhu. 2019. STING activation in
508 cancer immunotherapy. *Theranostics* 9: 7759-7771.

509 39. Amouzegar, A., M. Chelvanambi, J. N. Filderman, W. J. Storkus, and J. J. Luke. 2021.
510 STING Agonists as Cancer Therapeutics. *Cancers (Basel)* 13.

40. Le Naour, J., L. Zitvogel, L. Galluzzi, E. Vacchelli, and G. Kroemer. 2020. Trial watch: STING agonists in cancer therapy. *Oncoimmunology* 9: 1777624.

41. Zhang, W., and X. Huang. 2025. Targeting cGAS-STING pathway for reprogramming tumor-associated macrophages to enhance anti-tumor immunotherapy. *Biomark Res* 13: 43.

42. Wang, Q., K. Sudan, E. Schmoeckel, B. P. Kost, C. Kuhn, A. Vattai, T. Vilsmaier, S. Mahner, U. Jeschke, and H. H. Heidegger. 2022. CCL22-Polarized TAMs to M2a Macrophages in Cervical Cancer In Vitro Model. *Cells* 11.

43. Liu, Y., and F. Pu. 2023. Updated roles of cGAS-STING signaling in autoimmune diseases. *Front Immunol* 14: 1254915.

44. Gulen, M. F., N. Samson, A. Keller, M. Schwabenland, C. Liu, S. Gluck, V. V. Thacker, L. Favre, B. Mangeat, L. J. Kroese, P. Krimpenfort, M. Prinz, and A. Ablasser. 2023. cGAS-STING drives ageing-related inflammation and neurodegeneration. *Nature* 620: 374-380.

45. Faget, J., C. Biota, T. Bachelot, M. Gobert, I. Treilleux, N. Goutagny, I. Durand, S. Léon-Goddard, J. Y. Blay, C. Caux, and C. Ménétrier-Caux. 2011. Early detection of tumor cells by innate immune cells leads to T(reg) recruitment through CCL22 production by tumor cells. *Cancer Res* 71: 6143-6152.

46. Ma, F., B. Li, S. Y. Liu, S. S. Iyer, Y. Yu, A. Wu, and G. Cheng. 2015. Positive feedback regulation of type I IFN production by the IFN-inducible DNA sensor cGAS. *J Immunol* 194: 1545-1554.

47. Ma, F., B. Li, Y. Yu, S. S. Iyer, M. Sun, and G. Cheng. 2015. Positive feedback regulation of type I interferon by the interferon-stimulated gene STING. *EMBO Rep* 16: 202-212.

48. Blest, H. T. W., and L. Chauveau. 2023. cGAMP the travelling messenger. *Front Immunol* 14: 1150705.

49. Carozza, J. A., V. Bohnert, K. C. Nguyen, G. Skariah, K. E. Shaw, J. A. Brown, M. Rafat, R. von Eyben, E. E. Graves, J. S. Glenn, M. Smith, and L. Li. 2020. Extracellular cGAMP is a cancer cell-produced immunotransmitter involved in radiation-induced anti-cancer immunity. *Nat Cancer* 1: 184-196.

50. Mekers, V. E., V. M. Kho, M. Ansems, and G. J. Adema. 2022. cGAS/cGAMP/STING signal propagation in the tumor microenvironment: Key role for myeloid cells in antitumor immunity. *Radiother Oncol* 174: 158-167.

51. Ritchie, C., J. A. Carozza, and L. Li. 2022. Biochemistry, Cell Biology, and Pathophysiology of the Innate Immune cGAS-cGAMP-STING Pathway. *Annu Rev Biochem* 91: 599-628.

52. Wang, M., P. Xu, and Q. Wu. 2024. Cell-to-cell communications of cGAS-STING pathway in tumor immune microenvironment. *Zhejiang Da Xue Xue Bao Yi Xue Ban* 53: 15-24.

551 **FIGURE LEGENDS**

552

553 **Figure 1. STING activation in macrophages and monocytes does not upregulate CCL22.**
554 ***A)*** Microscopic images (20x brightfield) of THP-1 monocytes (upper left) and fully
555 differentiated THP-1-derived macrophages (lower right) are shown. ***B)*** THP-1-derived
556 macrophages were treated with cGAM(PS)2 (30 μM) for 24 hours, then harvested in TRIzol for
557 RNA purification and RTqPCR. Relative *CCL22* gene expression is shown. ***C)*** THP-1-derived
558 macrophages were treated with cGAM(PS)2 (30 μM) for 6 and 24 hours, then whole cell lysates
559 (20 μg) and antibody positive control (7 μg) were resolved with SDS-PAGE, transferred to
560 nitrocellulose, and probed for phosphorylated STING and beta-tubulin. ***D)*** THP-1 monocytes
561 were treated with cGAM(PS)2 (30 μM) and harvested for RTqPCR and *CCL22* gene expression
562 as described in *B*. Error bars represent standard deviations of independent biological replicates.
563 Statistical analyses were performed with unpaired, two-tailed *t* test (*B)* or non-parametric
564 Wilcoxon signed-rank test (*D*) due to non-Gaussian distribution of the treated sample per
565 Shapiro-Wilk test.

566

567 **Figure 2. STING-activated macrophages and monocytes release factor(s) that upregulate**
568 ***CCL22* in cancer cells.** ***A)*** MCF7 and ***B)*** HeLa cells were treated for 24 hours with cGAM(PS)2
569 (30 μM) or conditioned media (CM) from macrophages that were either untreated or treated with
570 cGAM(PS)2 (30 μM) for 24 hours prior to media collection. Cells were harvested with TRIzol
571 for RNA purification and RTqPCR to assess relative expression of *CCL22.* ***C)*** MCF7 and ***D)***
572 HeLa cells were treated for 24 hours with cGAM(PS)2 (30 μM) or conditioned media (CM) from
573 monocytes that were either untreated or treated with cGAM(PS)2 (30 μM) for 24 hours prior to

574 media collection. Cells were harvested with TRIzol for RNA purification and RTqPCR to
575 determine expression of *CCL22* as above. For all figures, error bars represent standard deviations
576 of independent biological replicates. Statistical analyses were performed with one-way ANOVAs
577 on log-transformed data and Tukey's pairwise comparisons (*A*, *C*, and *D*) or with Brown-
578 Forsythe and Welch ANOVA (*B*) due to significant differences among standard deviations.
579
580 **Figure 3. Paracrine activation of *CCL22* remains dependent on STING.** ***A)*** HeLa cells were
581 treated for 24 hours with cGAM(PS)2 (30 μM) or conditioned media (CM) from macrophages
582 that were either untreated or treated with cGAM(PS)2 (30 μM) for 24 hours. Whole cell lysates
583 (25 μg) and antibody positive control (5 μg) were resolved with SDS-PAGE, transferred to
584 nitrocellulose and probed for phosphorylated STING and beta-tubulin. The image shown is
585 representative of at least three independent experiments. ***B)*** HeLa$^{-/-\ TMEM173}$ STING knockout
586 cells were treated for 24 hours with cGAM(PS)2 (30 μM) or conditioned media (CM) from
587 macrophages that were either untreated or treated with cGAM(PS)2 (30 μM) for 24 hours prior
588 to media collection. Cells were harvested with TRIzol for RNA purification and RTqPCR to
589 determine relative expression of *CCL22*. Error bars represent standard deviations of independent
590 biological replicates. Statistical analysis was performed using one-way ANOVA and Tukey's
591 pairwise comparisons.
592
593 **Figure 4. Type I IFNs have modest effects on *CCL22* in HeLa cells that remain STING-**
594 **dependent.** HeLa ***(A-B)*** and MCF7 cells ***(C- D)*** were treated with exogenous type I IFNs at
595 indicated concentrations for 48 (HeLa) or 24 hours (MCF7), then harvested with TRIzol for
596 RNA purification and RTqPCR to determine relative gene expression of *CCL22*. ***E-F)*** HeLa $^{-/-}$

597 *TMEM173* STING knockout cells were treated with exogenous type I IFNs at indicated
598 concentrations for 48 hours, then harvested with TRIzol for RNA purification and RTqPCR
599 analysis of *CCL22.* Error bars represent standard deviations of independent biological replicates.
600 Statistical analyses were performed using one-way ANOVA with Dunnett's multiple
601 comparisons test (*A, C, E*), one-way ANOVA on log-transformed data with Tukey's pairwise
602 comparisons (*B, D*), and unpaired, two-tailed t test (*F*). ***G)*** HeLa wild type cells were treated
603 with IFNβ (100 ng/mL) for 48 hours, and whole cell lysates (60 μg) and antibody positive
604 control (5 μg) were resolved with SDS-PAGE, transferred to nitrocellulose and probed for
605 phosphorylated STING and beta-tubulin. ***H)*** HeLa wild type (WT) and HeLa *-/-TMEM173* STING
606 knockout (KO) cells were treated as indicated for approximately 30 hours prior to harvesting;
607 whole cell lysates (15 μg) were resolved with SDS-PAGE, transferred to nitrocellulose, and
608 probed for phosphorylated Stat1 and beta-tubulin. ***I)*** HeLa cells were pretreated for 3 hours with
609 MMHAR-2 neutralizing antibody, then indicated treatments were added, including conditioned
610 media (CM) from macrophages treated with cGAM(PS)2 (30 μM), and cells were incubated for
611 approximately 48 hours prior to harvest in TRIzol for RNA purification and RTqPCR to assess
612 relative changes in *CCL22* expression. Statistical analyses were performed using one-way
613 ANOVA with Šídák's multiple comparisons test.
614
615 **Figure 5. STING agonists differentially upregulate *CCL22* and *IFNβ*.** HeLa ***(A-D)*** and
616 MCF7 cells ***(E-H)*** were treated with 30 μM of each indicated STING agonist or DMSO vehicle
617 control (diABZI) for 24 hours, then harvested in TRIzol for RNA purification and RTqPCR.
618 Fold increases of gene expression for *CCL22* (closed circles) and *IFNβ* (open triangles) are
619 plotted relative to their respective untreated controls. Error bars represent standard deviations of

620 independent biological replicates. Statistical analyses were performed using one-way ANOVA
621 on log-transformed data and Dunnett's pairwise comparisons for all except panel *F*, which was
622 analyzed using the non-parametric Kruskal-Wallis test and Dunn's multiple comparisons due to a
623 non-Gaussian distribution of the *IFNβ* data. ***I)*** Correlation plot shows the relationship between
624 *IFNβ* and *CCL22* in MCF7 cells, with the Pearson r value shown.

Fig. 1

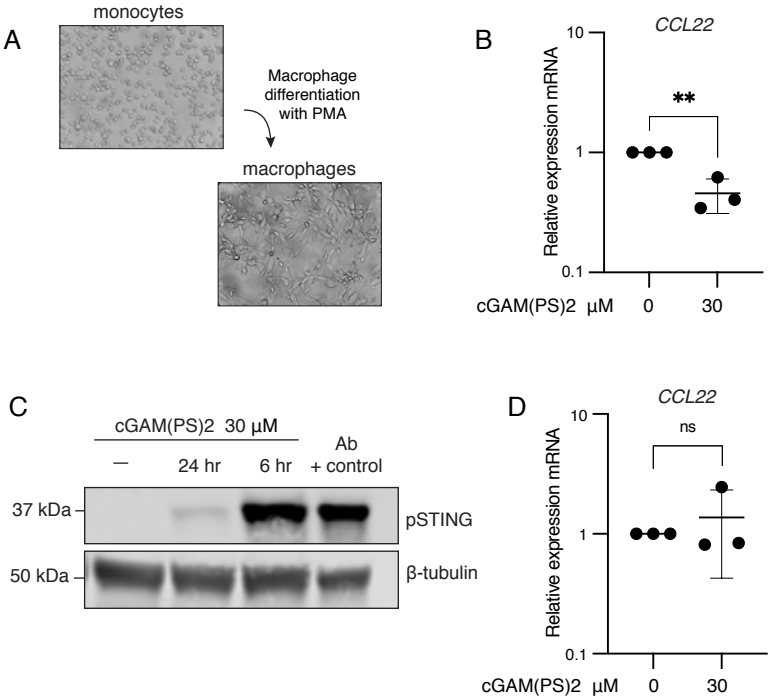
A
monocytes
Macrophage differentiation with PMA
macrophages
B
CCL22
Relative expression mRNA
10
1
0.1
**
cGAM(PS)2 μM
0
30
C
cGAM(PS)2 30 μM
—
24 hr
6 hr
Ab + control
37 kDa
pSTING
50 kDa
β-tubulin
D
CCL22
Relative expression mRNA
10
1
0.1
ns
cGAM(PS)2 μM
0
30

Fig. 2

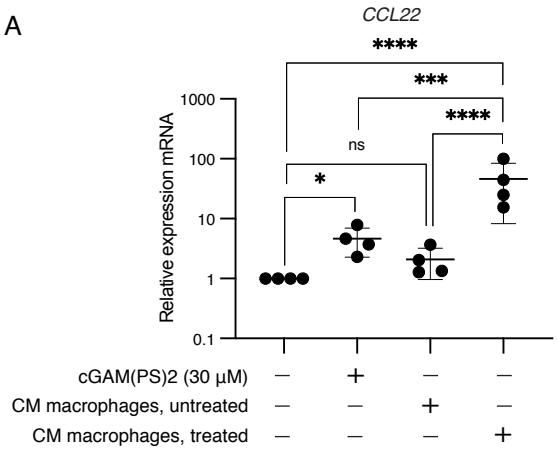
A
CCL22
****
***
****
ns
*
Relative expression mRNA
1000
100
10
1
0.1
cGAM(PS)2 (30 μM) – + – –
CM macrophages, untreated – – + –
CM macrophages, treated – – – +

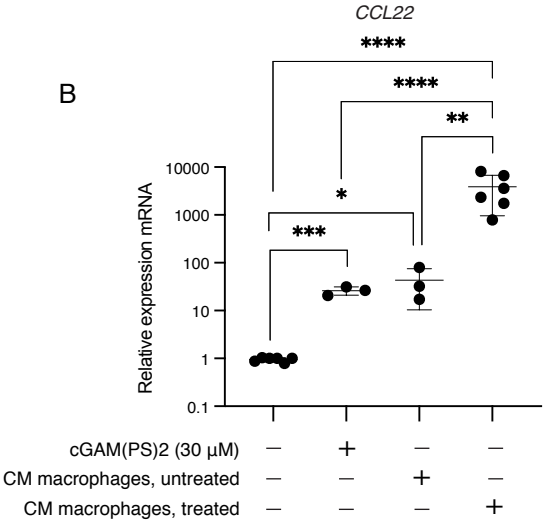
B
CCL22
****
****
**
*
***
Relative expression mRNA
10000
1000
100
10
1
0.1
cGAM(PS)2 (30 μM) – + – –
CM macrophages, untreated – – + –
CM macrophages, treated – – – +

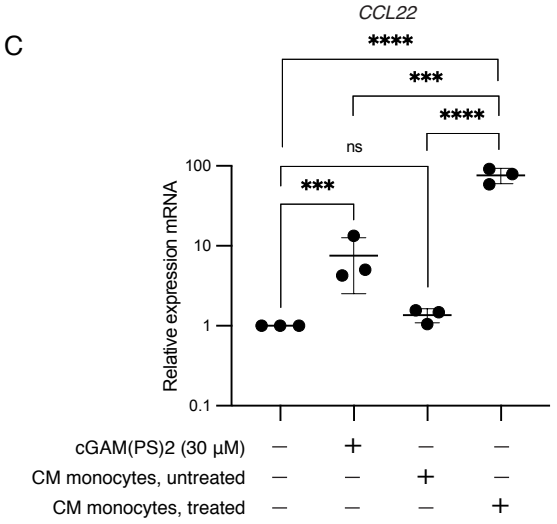
C
CCL22
****
***
****
ns
***
Relative expression mRNA
100
10
1
0.1
cGAM(PS)2 (30 μM) – + – –
CM monocytes, untreated – – + –
CM monocytes, treated – – – +

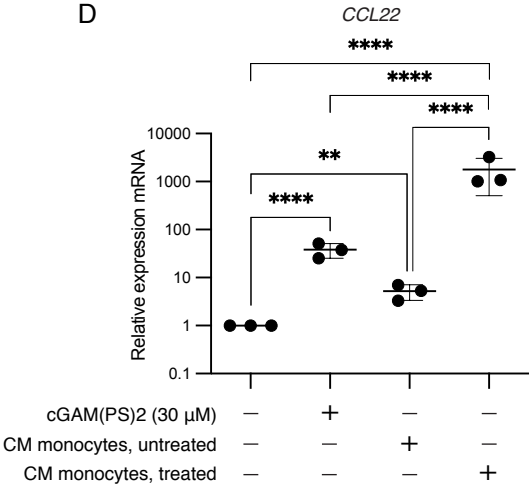
D
CCL22
****
****
****
**
****
Relative expression mRNA
10000
1000
100
10
1
0.1
cGAM(PS)2 (30 μM) – + – –
CM monocytes, untreated – – + –
CM monocytes, treated – – – +

Fig. 3

A

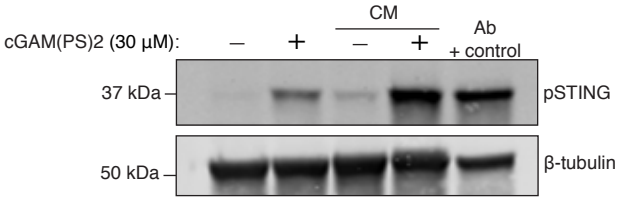
CM
cGAM(PS)2 (30 μM):
–
+
–
+
Ab
+ control
37 kDa
pSTING
50 kDa
β-tubulin

B

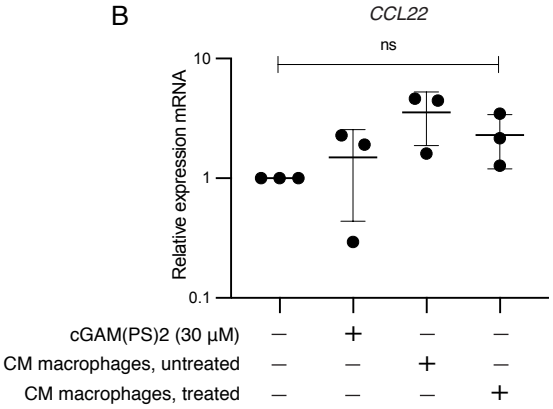
CCL22
ns
Relative expression mRNA
10
1
0.1
cGAM(PS)2 (30 μM)
CM macrophages, untreated
CM macrophages, treated

Fig. 4

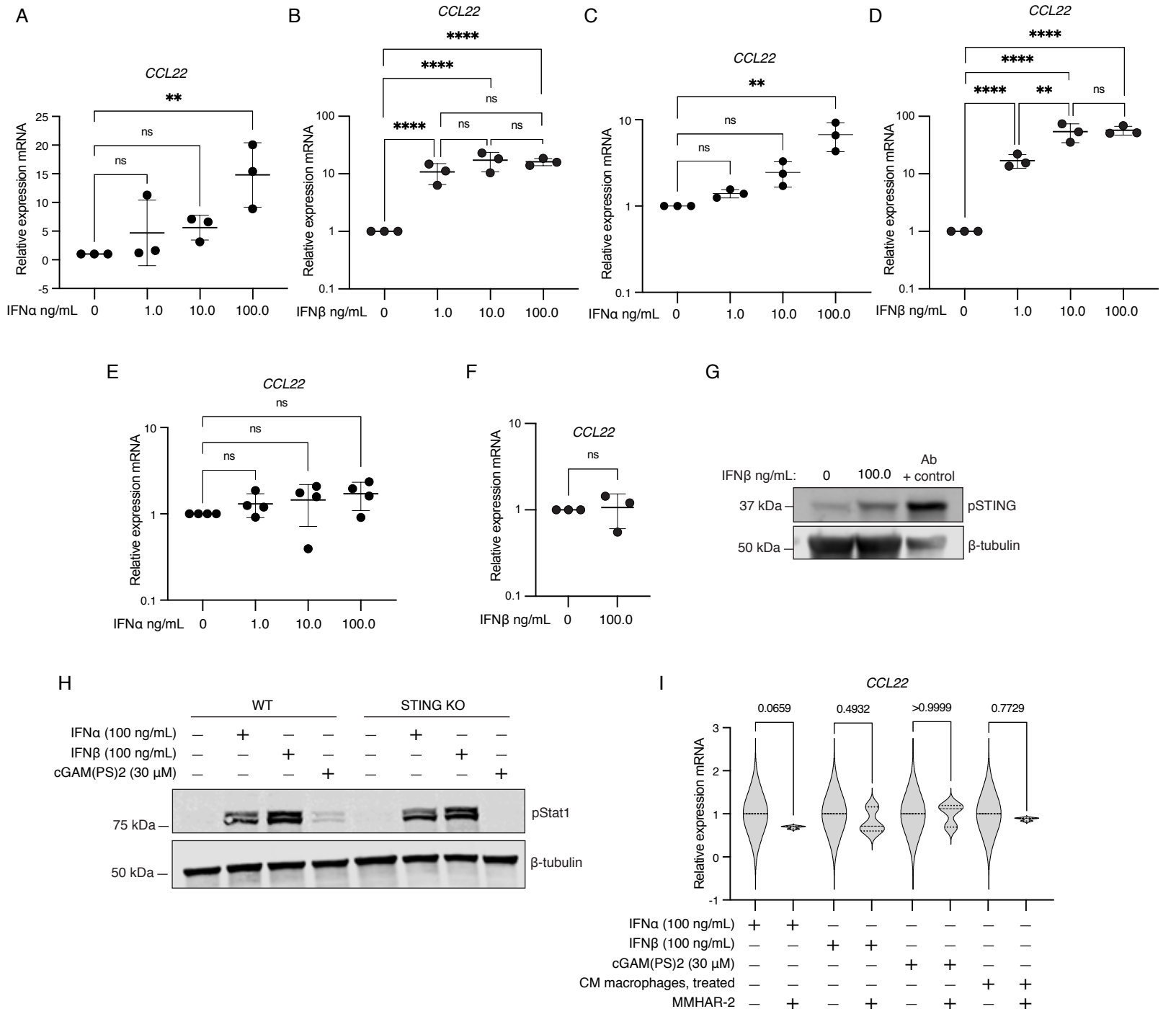
A
CCL22
Relative expression mRNA
IFNα ng/mL 0 1.0 10.0 100.0
B
CCL22
IFNβ ng/mL 0 1.0 10.0 100.0
C
CCL22
IFNα ng/mL 0 1.0 10.0 100.0
D
CCL22
IFNβ ng/mL 0 1.0 10.0 100.0
E
CCL22
IFNα ng/mL 0 1.0 10.0 100.0
F
CCL22
IFNβ ng/mL 0 100.0
G
IFNβ ng/mL: 0 100.0 Ab + control
37 kDa
pSTING
50 kDa
β-tubulin
H
WT
STING KO
IFNα (100 ng/mL)
IFNβ (100 ng/mL)
cGAM(PS)2 (30 μM)
75 kDa
pStat1
50 kDa
β-tubulin
I
CCL22
0.0659
0.4932
>0.9999
0.7729
Relative expression mRNA
IFNα (100 ng/mL)
IFNβ (100 ng/mL)
cGAM(PS)2 (30 μM)
CM macrophages, treated
MMHAR-2

Fig. 5

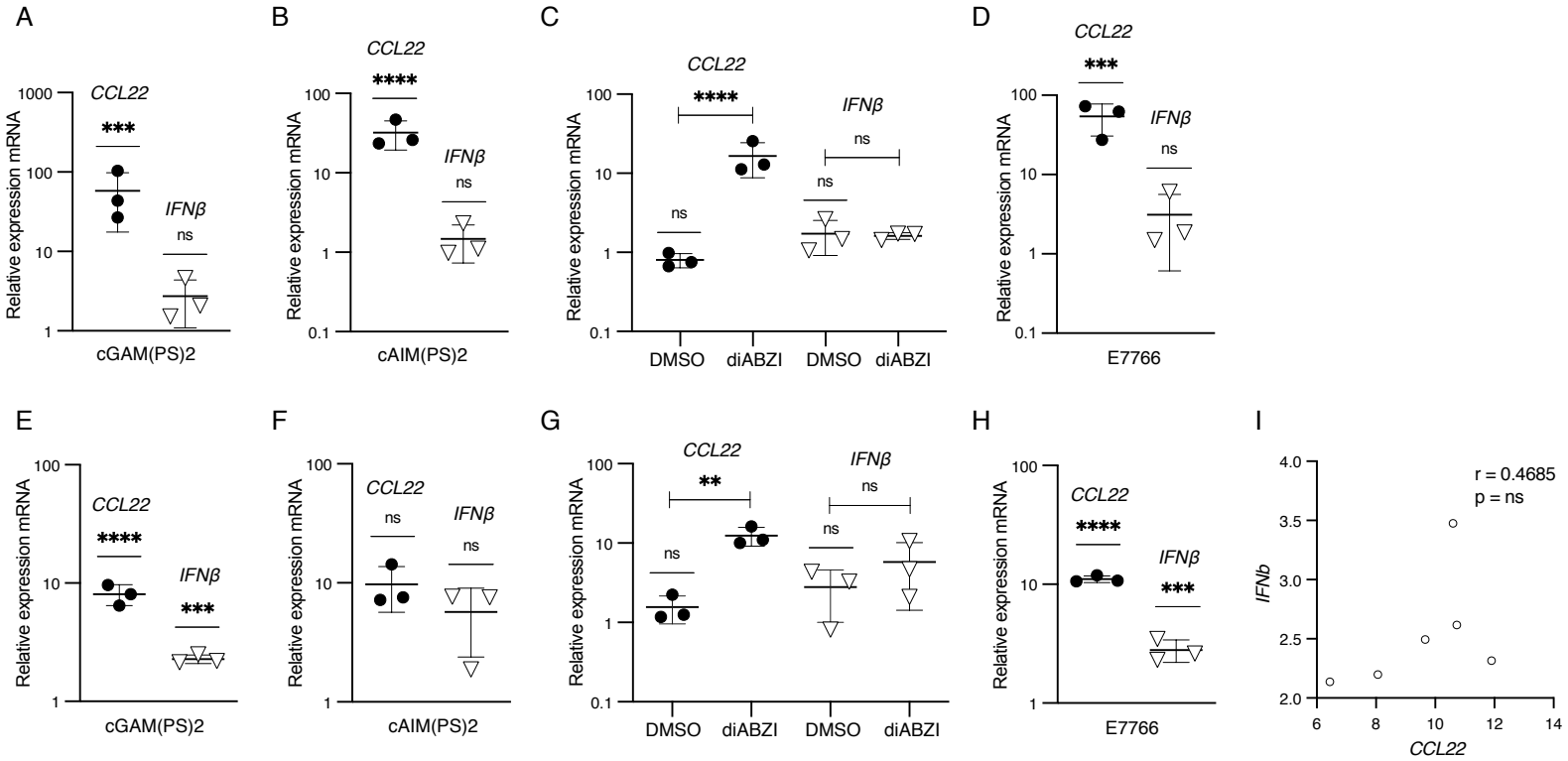
A
B
C
D
E
F
G
H
I
Relative expression mRNA
CCL22
IFNβ
***
****
ns
**
cGAM(PS)2
cAIM(PS)2
DMSO
diABZI
E7766
IFNb
r = 0.4685
p = ns